

Axion-like Dark Matter Constraints from CMB Birefringence

Günter Sigl

*Universität Hamburg, II. Institut für Theoretische Physik,
Luruper Chaussee 149, 22761 Hamburg, Germany**

Pranjal Trivedi

*Universität Hamburg, II. Institut für Theoretische Physik, Luruper Chaussee 149, 22761 Hamburg,
Hamburger Sternwarte, Gojenbergsweg 112, 21029 Hamburg, Germany;
Department of Physics, Sri Venkateswara College, University of Delhi 110020 India†*

Axion-like particles are dark matter candidates motivated by the Peccei-Quinn mechanism and also occur in effective field theories where their masses and photon couplings are independent. We estimate the dispersion of circularly polarized photons in a background of oscillating axion-like particles (ALPs) with the standard $g_{a\gamma} a F_{\mu\nu} \tilde{F}^{\mu\nu}/4$ coupling to photons. This leads to birefringence or the rotation of linear polarization that can constrain the axion-photon coupling $g_{a\gamma}$. The cosmic microwave background (CMB) polarization is a sensitive probe of cosmic birefringence arising from an effective refractive index that would be induced by ALP dark matter. The birefringence limit from CMB observations $\Delta\alpha \lesssim (0.5)^\circ$ enables us to constrain the axion-photon coupling $g_{a\gamma} \lesssim 10^{-18} - 10^{-13} \text{ GeV}^{-1}$, for ultra-light ALP masses $m_a \sim 10^{-27} - 10^{-22} \text{ eV}$. This represents an improvement of one to a few orders of magnitude upon the tightest prior limits derived from x-ray observations of active galaxies in clusters, although the techniques have different assumptions. Future CMB polarization experiments and their birefringence forecasts have the potential to further refine ALP dark matter parameters.

* guenter.sigl@desy.de

† pranjal.trivedi@desy.de

I. INTRODUCTION

Axion-like particles (ALPs) are generally understood as pseudoscalar fields a with a two-photon coupling of the form $g_{a\gamma} a F_{\mu\nu} \tilde{F}^{\mu\nu}/4$, among possible other couplings that are typically less relevant in dilute media. ALPs are generalizations of axions which were originally motivated by solving the strong CP problem through promoting the CP-violating phase θ to a/f_a with f_a known as the Peccei-Quinn scale [1–3]. Through its couplings to gluons and quarks the axion will attain a mass m_a below the QCD scale through which its expectation value is driven to zero.

Apart from the coupling constant $g_{a\gamma}$, ALPs are characterized through their vacuum mass m_a . In contrast to axions, ALPs in general do not solve the strong CP problem and $g_{a\gamma}$ and m_a are assumed to be independent parameters. In addition to the misalignment mechanism generating ALP cold dark matter, inflation also produces ALP field fluctuations of order the inflationary expansion rate, $H_i/(2\pi)$, which gives a contribution $\rho_a \sim m_a^2 H_i^2/(2\pi)^2$. For $m_a \gtrsim 3 \times 10^3 (10^{16} \text{ GeV}/H_i) H(z_{\text{rec}})$ and sufficiently large H_i , it can also lead to the right relic dark matter density.

The coupling term can lead to ALP-photon oscillations in the presence of external electromagnetic fields and also lead to an effective refractive index for photons propagating in a background of ALPs. While the former effect has been investigated extensively in both cosmological, astrophysical contexts (for reviews see Ref. [4, 5]) and in experiments (for a review see Ref. [6]), at least so far, the latter effect is less well studied. This refractive effect can be particularly relevant if ALPs constitute a significant part of the dark matter which is what we assume here without specifying the ALP production processes.

We investigate the birefringent effect of ALP dark matter on the cosmic microwave background (CMB) which is well constrained observationally. This leads to strong constraints on $g_{a\gamma}$ in the mass range $10^{-27} \text{ eV} \lesssim m_a \lesssim 10^{-22} \text{ eV}$, overlapping with the mass range of ultra-light and fuzzy dark matter [7] which has gained significant popularity recently. The constraints that already exist are generally flat in m_a for $m_a \lesssim 10^{-10} \text{ eV}$ and at the level $\sim 10^{-12} \text{ GeV}^{-1}$.

The linear polarization of the CMB is sourced by the quadrupole temperature anisotropy of the radiation field via Thomson scattering [8]. The curl-free E-mode polarization has been observed [9] with greater sensitivity and resolution in recent years by Planck [10] and several ground based experiments at higher resolution [11]. Steadily improving upper limits have also been placed on the gradient-free B-type polarization in the quest for the signal of inflationary tensor modes [12]. The birefringence of the linear polarization of the CMB, arising due to any parity violation [13–16], can be probed via correlations of the E and B-modes [15, 17, 18]. In this work we ignore clustering of ALP dark matter [5] and anisotropies in the birefringence [19–21]. The goal of this paper is to calculate the overall amplitude of birefringence predicted by an oscillating background of ALP dark matter and use the observational limits on CMB birefringence to constrain the axion-photon coupling constant as a function of ALP mass.

II. PHOTON PROPAGATION IN AN ALP BACKGROUND

Using natural units $c = \hbar = k_B = 1$ and Lorentz-Heaviside units $\epsilon_0 = \mu_0 = 1$, the parts of the Lagrangian depending on the ALP and photon fields can be written as

$$\mathcal{L}_{a\gamma} = -\frac{1}{4} F_{\mu\nu} F^{\mu\nu} + \frac{1}{2} \partial_\mu a \partial^\mu a + \frac{1}{4} g_{a\gamma} a F_{\mu\nu} \tilde{F}^{\mu\nu} - V_a(a), \quad (1)$$

where $F_{\mu\nu}$ is the electromagnetic field strength tensor, $\tilde{F}_{\mu\nu}$ is its dual and $V_a(a)$ is the effective ALP potential which can be expanded as $V_a(a) = \frac{1}{2} m_a^2 a^2 + \mathcal{O}(a^3)$ around $a = 0$, with m_a the effective ALP mass. One often uses the relation

$$g_{a\gamma} = \frac{s \alpha_{\text{em}}}{2\pi f_a}, \quad (2)$$

with s a model dependent parameter of order unity, α_{em} the fine structure constant and f_a the Peccei-Quinn scale. For left- and right-circular photon modes propagating in the z -direction we make the Ansatz

$$\mathbf{A}_\pm(t, \mathbf{r}) = A_\pm(t) \mathbf{e}_\pm e^{ikz}, \quad (3)$$

where $\mathbf{e}_\pm \equiv \mathbf{e}_x \pm i\mathbf{e}_y$ are the two unit vectors corresponding to left and right-circular modes. To zeroth order, photon wave-packets will propagate along trajectories $z = t$ so that we can identify time scales with length scales from now on. Eq. (3) then yields the equation of motion

$$\left(\frac{\partial^2}{\partial t^2} + k^2 \right) A_\pm(t) = \pm \frac{k m_a g_{a\gamma}}{\epsilon_0} a_0 \cos(m_a t + \delta) A_\pm(t), \quad (4)$$

where δ is a random phase which changes on the length scale of the coherence length l_c of the ALP field and a_0 is the amplitude of the ALP field which is supposed to vary on time and lengths scales much larger than $1/k$ and the inverse photon frequency. Eq. (4) is of the form of a Mathieu equation. It can be brought into its standard form (up to the phase δ)

$$\left[\frac{d^2}{dx^2} + A - 2q \cos(2x + \delta) \right] y(x) = 0 \quad (5)$$

via the substitutions

$$x \equiv m_a t/2, \quad A = \frac{4k^2}{m_a^2}, \quad q = \pm \frac{2kg_{a\gamma}}{\epsilon_0} \frac{a_0}{m_a} \simeq \pm 5.5 \times 10^{-19} (g_{a\gamma} 10^{14} \text{ GeV}) \left(\frac{\mu\text{eV}}{m_a} \right) \left(\frac{k}{m_a} \right) \left(\frac{\rho_a}{0.3 \text{ GeV/cm}^3} \right)^{1/2}.$$

For the ALP amplitude a_0 we use the relation $\rho_a = (1/2)m_a^2 a_0^2$, and set $\rho_a \simeq 0.3 \text{ GeV cm}^{-3}$ for the standard average Galactic dark matter density. The ALP fraction of dark matter can be constrained to 0.2 at $m_a \lesssim 10^{-22} \text{ eV}$ from the Lyman- α forest [22, 23]. However, for ease of comparison, we assume all dark matter to be in the form of ALPs and we also find our constraints on $g_{a\gamma}$ depend rather weakly on matter density.

III. BIREFRINGENCE PHASE SHIFT AND AXION-PHOTON COUPLING

For sufficiently small ALP masses m_a , the cosine can be treated as constant on macroscopic scales $\simeq 1/m_a$. In this case, Eq. (4) leads to the dispersion relation

$$\omega = k \mp \frac{m_a g_{a\gamma}}{2\epsilon_0} a_0 \cos(m_a t + \delta). \quad (6)$$

This can be also be written as $\Delta\phi = \Delta\omega dt \sim g_{a\gamma} \Delta a$ which is the same as e.g. Eq.(2) in [24]. Note our $g_{a\gamma}$ is their $1/f_a$ without the factors in our Eq.(2). Using $k = m_a/2$, a single domain or coherence length l_c of the ALP field gives rise to the phase difference between the left and right-circularly polarized photon modes of the order

$$\Delta\phi_1 \simeq |q| \simeq \frac{g_{a\gamma}}{\epsilon_0} a_0 \simeq 2.1 \times 10^{-4} (g_{a\gamma} 10^{14} \text{ GeV}) \left(\frac{10^{-22} \text{ eV}}{m_a} \right) \left(\frac{\rho_a}{0.3 \text{ GeV/cm}^3} \right)^{1/2} \text{ rad}. \quad (7)$$

The coherence length l_c is roughly the de Broglie wavelength of the ALP, $l_c \sim 1/(m_a v_a)$. The phase shift accumulated over a coherence length l_c does not depend on l_c as long as $l_c \gtrsim 1/m_a$ because $\int_0^{l_c} dz \cos(m_a t + \delta) \simeq [\sin(m_a l_c + \delta) - \sin(\delta)]/m_a = \mathcal{O}(1/m_a)$. Furthermore, $\Delta\phi_1$ does not depend on the photon frequency (unlike Faraday rotation) so that observations in any wavelength band can be applied! On the other hand, over distances $d \lesssim l_c$ the accumulated phase shift would be a factor d/l_c smaller than Eq. (7).

The accumulated cosmological phase shift as photons traverse ALP-field coherent domains (of number N), between the surface of last scattering at recombination and the present epoch, can be estimated by integrating over domains to get the mean square phase shift

$$\begin{aligned} (\Delta\phi)^2 &\simeq \left(\frac{g_{a\gamma}}{\epsilon_0} \right)^2 \int dN \frac{a_0^2(t)}{2} = \left(\frac{g_{a\gamma}}{\epsilon_0} \right)^2 \int_0^{t_{\text{rec}}} dt m_a v_a(t) \frac{a_0^2(t)}{2} \\ &= \left(\frac{g_{a\gamma}}{\epsilon_0} \right)^2 m_a \int_0^{z_{\text{rec}}} \frac{dz}{(1+z)H(z)} \frac{\rho_a(z) v_a(z)}{m_a^2} = \left(\frac{g_{a\gamma}}{\epsilon_0} \right)^2 \frac{\Omega_c \rho_{\text{crit}}}{m_a H_0} \int_0^{z_{\text{rec}}} \frac{dz}{(1+z)E(z)} (1+z)^3 v_a(z) \end{aligned} \quad (8)$$

where $H(z) = H_0 E(z) \simeq H_0 \sqrt{\Omega_m} (1+z)^{3/2}$ for $z_{\text{rec}} \gtrsim z \gg 1$, neglecting the small contribution from low- z dominated by dark energy. Using matter densities from [10] and in our units, $\epsilon_0 = 1$,

$$(\Delta\phi)^2 \simeq 7.1 \times 10^{-3} (g_{a\gamma} \cdot 10^{14} \text{ GeV})^2 \left(\frac{10^{-22} \text{ eV}}{m_a} \right) \left(\frac{\Omega_c}{0.264} \right) \left(\frac{0.7}{h} \right) \int_0^{z_{\text{rec}}} dz v_a(z) \frac{(1+z)^2}{E(z)} \text{ rad}^2. \quad (9)$$

The recombination era contribution $[2v_a(z_{\text{rec}})/3\sqrt{\Omega_m}](1+z)^{3/2}$ dominates the integral to give

$$(\Delta\phi)^2 \gtrsim 3.1 \times 10^{-2} (g_{a\gamma} \cdot 10^{14} \text{ GeV})^2 \left(\frac{10^{-22} \text{ eV}}{m_a} \right) \left(\frac{\Omega_c}{0.264} \right) \left(\frac{0.315}{\Omega_m} \right)^{1/2} \left(\frac{0.7}{h} \right) \left(\frac{v_a(z_{\text{rec}})}{10^{-4}} \right) \left(\frac{1+z_{\text{rec}}}{1100} \right)^{3/2} \text{ rad}^2, \quad (10)$$

CMB Experiment	Frequency (GHz)	Multipole-range	$\Delta\alpha$ (degrees)	$\Delta\alpha$ Reference	$g_{a\gamma}$
WMAP7	41,61,94	2-800	$-1.1 \pm 1.4 (\pm 1.5)$	Komatsu et al.(2011) [26]	42
POLARBEAR	148	500-2700	$-1.08 \pm 0.20 (\pm 0.5)$	POLARBEAR (2015) [27]	18
ACTpol	146	250-3025	$0.29 \pm 0.28 (\pm 0.5)$	Molinari et al. (2016) [28]	11
Planck	30-857 (9 ch.)	2-1500	$0.31 \pm 0.05 (\pm 0.28)$	Planck (2016) XLIX [29]	6.8
BICEP2/Keck	150	30-300	0.33	BICEP2/Keck Array IX (2017) [30]	3.5
<i>Current status</i>			0.5	<i>Limit adopted for this work</i>	5.3
(CMB-S4)	35-250	$\lesssim 10^4$	3×10^{-2}	CMB-S4 Science Book (2016) [31]	0.31
(CORe)	135 (60-600)	$\lesssim 1400$	3×10^{-3}	Molinari et al. (2016) [28]	0.031
(CV-limited $r=0.1$)		$\lesssim 3000$	10^{-5}	Molinari et al. (2016) [28]	10^{-4}

TABLE I. Comparison of observed limits and forecasts on birefringence angle α from various CMB experiments (and a cosmic variance-limited case) along with their relevant frequency and multipole range. The last column contains the upper-limit constraint on axion-photon coupling $g_{a\gamma}$ ($\times 10^{-17}$ GeV $^{-1}$) derived from Eq. (13), evaluated at $m_a = m_{a,\text{coh}} = 3 \times 10^{-25}$ eV.

which results in an r.m.s. phase shift (averaged over the sky),

$$\Delta\phi_{\text{rms}} \gtrsim 0.17 (g_{a\gamma} \cdot 10^{14} \text{GeV}) \left(\frac{10^{-22} \text{eV}}{m_a} \right)^{1/2} \left(\frac{\Omega_c}{0.264} \right)^{1/2} \left(\frac{0.315}{\Omega_m} \right)^{1/4} \left(\frac{0.7}{h} \right)^{1/2} \left(\frac{v_a(z_{\text{rec}})}{10^{-4}} \right)^{1/2} \left(\frac{1+z_{\text{rec}}}{1100} \right)^{3/4} \text{rad.} \quad (11)$$

We adopt a value $v_a(z_{\text{rec}}) \sim 10^{-4}$ for the post-recombination axion velocity from estimates of the CDM velocity [25]. The random walk treatment breaks down if the ALP coherence length is larger than the Hubble radius at recombination $1/(m_a v_a(z_{\text{rec}})) \gtrsim 1/H(z_{\text{rec}})$ i.e. ($m_a \lesssim H(z_{\text{rec}})/v_a(z_{\text{rec}})$ which occurs at

$$m_{a,\text{coh}} \simeq 3 \times 10^{-25} \left(\frac{\Omega_m}{0.315} \right)^{1/2} \left(\frac{0.7}{h} \right)^{1/2} \left(\frac{v_a(z_{\text{rec}})}{10^{-4}} \right)^{-1} \left(\frac{1+z_{\text{rec}}}{1100} \right)^{3/2} \text{eV.} \quad (12)$$

The observed birefringence angle $\Delta\alpha$ (the angle of rotation of linear polarization) is half the phase shift $\Delta\phi$ between the two components of circular polarization. Observed and forecast limits on the birefringence angle from observations of the CMB are listed in Table I. The rotation of polarization (and its angular power spectrum) can be extracted via measuring E and B-mode polarization correlations [17] which arise when there is statistical parity violation, in our case sourced by the pseudoscalar axion field. For constraints on the axion-photon coupling, we adopt a current limit on $\Delta\alpha \lesssim (0.5)^\circ$ lying between the weaker Planck & ACTpol limits and tighter BICEP2/Keck Array limits. This produces an upper limit on the axion-photon coupling,

$$g_{a\gamma} \lesssim 5.3 \times 10^{-17} \left(\frac{\Delta\alpha}{(0.5)^\circ} \right) \left(\frac{m_a}{3 \times 10^{-25} \text{eV}} \right)^{1/2} \left(\frac{0.264}{\Omega_c} \right)^{1/2} \left(\frac{\Omega_m}{0.315} \right)^{1/4} \left(\frac{h}{0.7} \right)^{1/2} \left(\frac{10^{-4}}{v_a(z_{\text{rec}})} \right)^{1/2} \left(\frac{1100}{1+z_{\text{rec}}} \right)^{3/4} \text{GeV}^{-1}, \quad (13)$$

evaluated at $m_a = m_{a,\text{coh}}$.

We define $m_{a,\text{rec}} \sim H(z_{\text{rec}}) \sim 3 \times 10^{-29}$ eV, representing the lower limit of ALP mass that can oscillate at recombination. For the range of ALP masses $m_{a,\text{rec}} \lesssim m_a \lesssim m_{a,\text{coh}}$, the de Broglie wavelength is larger than the Hubble scale at recombination and the latter sets the effective coherence length. The phase shift will be given by Eq.(7) in this regime, $\Delta\phi_1 \simeq g_{a\gamma} a_0$ while $a_0 \propto 1/m_a$ so $g_{a\gamma} \propto m_a$ in this regime (whereas at $m_a \gtrsim m_{a,\text{coh}}$ it scales $g_{a\gamma} \propto m_a^{1/2}$). We ignore even smaller masses $m_a \lesssim H(z_{\text{rec}})$ as the ALP would not oscillate at recombination and act as dark energy till $H(z < z_{\text{rec}}) \lesssim m_a$. Also, the temperature-independent limit for ALP dark matter [33] is $m_a \gtrsim 7 \times 10^{-28}$ eV.

While our constraint for $g_{a\gamma}$ scales as $m_a^{1/2}$ and m_a , above and below $m_{a,\text{coh}}$, respectively, we can further specify the range of ALP masses probed by CMB experiments. The multipole ℓ of the signal is $\ell \sim \pi/\theta \sim \pi d_A/l_c \sim \pi d_A m_a v_a(z_{\text{rec}}) \sim 2\pi m_a v_a(z_{\text{rec}}/[H_0(1+z_{\text{rec}})])$, where d_A is the angular diameter distance. Therefore, the range of masses for a multipole range $\ell_{\text{range}} \sim 1 - 10^3$ is given by $[\ell_{\text{range}} H_0(1+z_{\text{rec}})]/[2\pi v_a(z_{\text{rec}})]$ expressed as $2.6 \times 10^{-27} \lesssim m_a \lesssim 2.6 \times 10^{-24}$ eV. The $g_{a\gamma}$ excluded over this mass range is depicted by the filled red region in Fig. 1.

We note that our upper limit $g_{a\gamma} \lesssim 5 \times 10^{-17}$ GeV $^{-1}$ at $m_{a,\text{coh}} \sim 3 \times 10^{-25}$ eV is $\sim 10^4$ times stronger than several limits from x-ray oscillations from AGN in magnetized clusters (3C 84 or NGC 1275 in the Perseus cluster [34] or M 87 [35]) and even $\sim 10^3$ times stronger than the forecast limit from Athena [36]. However, it must be emphasized that x-ray and CMB limits depend on different assumptions - the x-ray limits do not depend on ALP

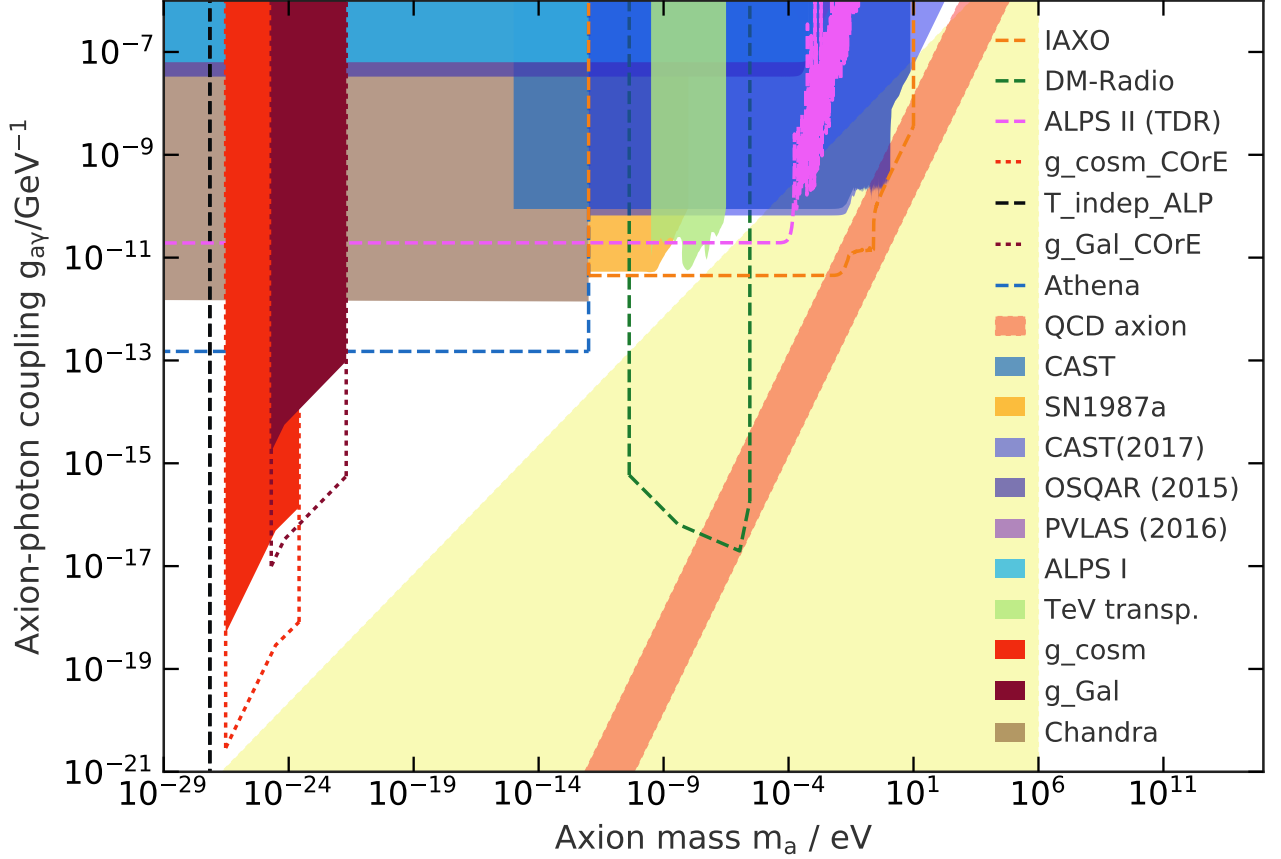


FIG. 1. Axion-photon coupling constant $g_{a\gamma}$ as a function of axion (ALP) dark matter mass. The constraints on $g_{a\gamma}$ derived in this work from Eq. (13) (filled red, labelled ‘g_cosm’) improve substantially on x-ray bounds from Chandra (filled brown) and forecasts for Athena (blue dashed line). Note that the x-ray limits are independent of ALP dark matter mass and assume a 25 μG cluster center magnetic field. Also shown is the Galactic constraint derived in this work (filled maroon, labelled ‘g_Gal’). Dotted lines indicate how future CMB observations from CoRE could improve $g_{a\gamma}$ constraints by two orders of magnitude (also similar to SKA 2 radio source forecasts). Other filled regions depict coupling constant-ALP mass parameter space already excluded by various other experiments and observations (some of them based on ALP-photon oscillations independent of dark matter). Dashed lines indicate forecasted constraints from various future experiments except the vertical black dashed line which indicates the limits of ALP dark matter (T-independent at 7×10^{-28} eV). The yellow filled region depicts the allowed parameter space for temperature-dependent ALP dark matter via the misalignment mechanism and the light red band with unit slope depicts QCD axion models (This plot was created using the ALPlot code [32]).

dark matter mass and assume a 25 μG cluster center magnetic field for Primakoff conversion. Our constraint is also ~ 30 times stronger than the constraint from polarized emission from a nearby protoplanetary disk [37]. CMB polarization constraints are also expected to be more robust than other methods as the predicted CMB polarization characteristics are theoretically well established and unaffected by astrophysical uncertainties in individual sources used in other methods. Cosmological models accurately fit sensitive all-sky observations by Planck [11, 29] as well as higher-resolution ground based experiments (e.g. see Table I) making tight limits on birefringence more reliable.

The birefringence analysis for deriving limits on $g_{a\gamma}$ from cosmological domains of oscillating ALPs can be repeated for the case of axions only in our Galactic potential with velocity dispersion $v_{a,\text{Gal}} \sim 10^{-3}$ and out to a distance $d_{\text{Gal}} \sim 10$ kpc. We find, as expected, the Galactic birefringence signal and its constraints on $g_{a\gamma}$ are weaker by about two orders of magnitude. The characteristic ALP mass scale in this case is $m_{a,\text{Gal}} \sim 1/(d_{\text{Gal}}v_{a,\text{Gal}}) \sim 6.7 \times 10^{-25}$ eV. The coupling constant constraint at $m_{a,\text{Gal}}$ is $g_{a\gamma} \lesssim 5.6 \times 10^{-15}$ GeV^{-1} and as before, it scales as $m_a^{1/2}$ and m_a , above and below $m_{a,\text{Gal}}$, respectively, as shown in Fig. 1. The Galactic ALP mass range probed by CMB observations within $\ell_{\text{range}} \sim 1 - 10^3$ is $2 \times 10^{-25} \lesssim m_a \lesssim 2 \times 10^{-22}$ eV for $d \sim 10$ kpc. Overall, we see that although the Galactic signal is almost 10^2 weaker in its constraint but it can probe up to 10^2 times higher m_a scales compared to the extragalactic and is depicted by the filled maroon region in Fig. 1. The Galactic contribution would also imprint birefringence anisotropy.

Future CMB observations have the promise of greatly reducing the r.m.s. amplitude of the polarization rotation angle (Table I). Controlling polarization-angle calibration systematics [38, 39], currently at the level of $(0.3)^\circ$, will be crucial to achieving the ~ 20 to 200 times tighter α limits [28] and $g_{a\gamma}$ limits that we forecast for the CMB-S4 and COrE-like experiment.

We should note that rotation angles of the polarized synchrotron emission from radio galaxies [14, 40] as well as scattered UV emission from extragalactic sources [41] can also constrain the birefringence rotation angle to approximately 1 degree. Such sources have the disadvantages of having to correct for Faraday rotation, projections effects and differing intrinsic polarization properties. However, with a future SKA 2 survey of $\sim 10^6$ polarized sources, a much improved overall rotation angle error of as low as 2×10^{-3} degree has been forecast (similar to COrE) for $\ell_{\max} \sim 700$ [42].

IV. CONCLUSIONS

We have demonstrated that the interaction of radiation propagating in an oscillating ALP dark matter background results in an accumulated rotation in the photon linear polarization (or phase shift between the two photon circular polarizations) which can be utilized to place constraints on the axion-photon coupling $g_{a\gamma}$. The photon dispersion relation contains a term oscillating in time with amplitude proportional to the strength of the axion-photon coupling constant $g_{a\gamma}$. The birefringence produced is achromatic i.e. independent of frequency.

We evaluated the total r.m.s. polarization rotation angle for CMB polarization by adding in quadrature the individual phase shifts over coherent patches of a size determined by the ALP's de Broglie wavelength $l_c \sim 1/(m_a v_a)$. The CMB provides a well-characterized all-sky distant polarization screen to probe against for this small polarization rotation. We derive different scalings for the coupling $g_{a\gamma}$, proportional to m_a and $m_a^{1/2}$, below and above the coherent mass scale at recombination. Using the current limit on birefringence angle of $(0.5)^\circ$ we place a constraint on the axion-photon coupling $g_{a\gamma} \lesssim 5 \times 10^{-17} \text{ GeV}^{-1}$ at $3 \times 10^{-25} \text{ eV}$. At this ALP mass scale, our limit improves on x-ray bounds from Chandra by \sim four orders of magnitude and the Athena forecast by three orders, although x-ray constraints are independent of dark matter ALP mass. Although Lyman- α forest observations [22, 23] can constrain the ALP dark matter fraction, our constraints scale as $g_{a\gamma} \propto \Omega_m^{-1/4}$ and will weaken by less than a factor of 1.5.

Our cosmological probe of ALPs via their effective refractive index is also quite complementary to helioscopes, haloscopes and light-shining-through-walls experiments in the ALP coupling vs. mass parameter space. Recently, sensitive laboratory measurements have been proposed to measure the same birefringence effect in the opposite small-scale limit [43]. In the future, CMB experiments and missions like CMB-S4 and COrE have the potential to additionally constrain $g_{a\gamma}$ by one and two orders of magnitude, respectively, at $3 \times 10^{25} \text{ eV}$.

Note Added: During preparation of this paper for submission we note that Reference [37] appeared which develops an analogous idea but in a different context of protoplanetary disks.

ACKNOWLEDGMENTS

This work has been supported by the Deutsche Forschungsgemeinschaft through the Collaborative Research Center SFB 676 “Particles, Strings and the Early Universe”. We acknowledge useful conversations with Robi Banerjee, Matthias Koschnitzke, Jens Niemeyer, Andreas Pargner, Georg Raffelt, Javier Redondo and Andreas Ringwald.

-
- [1] R. D. Peccei and H. R. Quinn, Phys. Rev. Lett. **38**, 1440 (1977).
 - [2] S. Weinberg, Phys. Rev. Lett. **40**, 223 (1978).
 - [3] F. Wilczek, Phys. Rev. Lett. **40**, 279 (1978).
 - [4] P. Arias *et al.*, J. Cosmol. Astropart. Phys. **6**, 013 (2012).
 - [5] D. J. E. Marsh, Phys. Rep. **643**, 1 (2016).
 - [6] I. G. Irastorza and J. Redondo, Progress in Particle and Nuclear Physics **102**, 89 (2018).
 - [7] L. Hui, J. P. Ostriker, S. Tremaine, and E. Witten, Phys. Rev. D **95**, 043541 (2017).
 - [8] W. Hu and S. Dodelson, Annual. Rev. Astron. Astrophys. **40**, 171 (2002).
 - [9] J. M. Kovac *et al.*, Nature (London) **420**, 772 (2002).
 - [10] Planck Collaboration *et al.*, ArXiv e-prints (2018).
 - [11] S. Staggs, J. Dunkley, and L. Page, Reports on Progress in Physics **81**, 044901 (2018).
 - [12] M. Kamionkowski and E. D. Kovetz, Annual Review of Astronomy and Astrophysics **54**, 227 (2016).
 - [13] S. M. Carroll, G. B. Field, and R. Jackiw, Phys. Rev. D **41**, 1231 (1990).

- [14] S. M. Carroll, Phys. Rev. Lett. **81**, 3067 (1998).
- [15] F. Finelli and M. Galaverni, Phys. Rev. D **79**, 063002 (2009).
- [16] M. Giovannini, Phys. Rev. D **71**, 021301 (2005).
- [17] M. Kamionkowski, Physical Review Letters **102**, 111302 (2009).
- [18] A. P. S. Yadav, M. Shimon, and B. G. Keating, Phys. Rev. D **86**, 083002 (2012).
- [19] V. Gluscevic, D. Hanson, M. Kamionkowski, and C. M. Hirata, Phys. Rev. D **86**, 103529 (2012).
- [20] D. Contreras, P. Boubel, and D. Scott, J. Cosmol. Astropart. Phys. **12**, 046 (2017).
- [21] G.-C. Liu and K.-W. Ng, Physics of the Dark Universe **16**, 22 (2017).
- [22] T. Kobayashi *et al.*, Phys. Rev. D **96**, 123514 (2017).
- [23] V. Iršič *et al.*, Physical Review Letters **119**, 031302 (2017).
- [24] M. Pospelov, A. Ritz, and C. Skordis, Physical Review Letters **103**, 051302 (2009).
- [25] D. Tseliakhovich and C. Hirata, Phys. Rev. D **82**, 083520 (2010).
- [26] E. Komatsu *et al.*, Astrophys. J. S. **192**, 18 (2011).
- [27] P. A. R. Ade *et al.*, Phys. Rev. D **92**, 123509 (2015).
- [28] D. Molinari, A. Gruppuso, and P. Natoli, Physics of the Dark Universe **14**, 65 (2016).
- [29] Planck Collaboration *et al.*, Astron. Astrophys. **594**, A11 (2016).
- [30] BICEP2 Collaboration *et al.*, Phys. Rev. D **96**, 102003 (2017).
- [31] K. N. Abazajian *et al.*, ArXiv e-prints (2016).
- [32] ALPlot, Lichtenberg Research Group, University Mainz,, <https://alplot.physik.uni-mainz.de>.
- [33] M. Tanabashi *et al.*, Physical Review D **98**, (2018).
- [34] M. Berg *et al.*, Astrophys. J. **847**, 101 (2017).
- [35] M. C. D. Marsh *et al.*, J. Cosmol. Astropart. Phys. **12**, 036 (2017).
- [36] J. P. Conlon *et al.*, Mon. Not. R. Astron. Soc. **473**, 4932 (2018).
- [37] T. Fujita, R. Tazaki, and K. Toma, ArXiv e-prints (2018).
- [38] J. P. Kaufman, B. G. Keating, and B. R. Johnson, Mon. Not. R. Astron. Soc. **455**, 1981 (2016).
- [39] N. J. Miller, M. Shimon, and B. G. Keating, Phys. Rev. D **79**, 063008 (2009).
- [40] J. P. Leahy, ArXiv Astrophysics e-prints (1997).
- [41] S. di Serego Alighieri, F. Finelli, and M. Galaverni, Astrophys. J. **715**, 33 (2010).
- [42] L. Whittaker, R. A. Battye, and M. L. Brown, Mon. Not. R. Astron. Soc. **474**, 460 (2018).
- [43] H. Liu, B. D. Elwood, M. Evans, and J. Thaler, ArXiv e-prints (2018).